


A simple mechanical model for simulating cross-country skiing, skating technique

John Bruzzo¹  · A. L. Schwab² · Antti Valkeapää¹ · Aki Mikkola¹ · Olli Ohtonen³ · Vesa Linnamo³

© International Sports Engineering Association 2015

Abstract The role of simulation models in sport disciplines has become relevant lately due to the multiple advantages that they may offer sports teams, coaches and practitioners. This paper develops and presents a simple three-dimensional multibody dynamic model of a cross-country skier, modeling a single propulsion phase to obtain the kinetic parameters involved in the movement. A professional Olympic-level skier performed the skating technique without poles in a ski tunnel under controlled conditions and on an incline plane. Then, with a force acquisition system attached to the ski bindings and a motion capture system set on site, the leg resultant forces and the movement of specific points of the skier's lower body were acquired. The data obtained from the motion capture system were used as the prescribed kinematic input data in the multibody model and the measured force was used later as a parameter of comparison with the results of the simple model. After simulating the technique, the calculated resultant forces seem to be in agreement with those measured in the field.

Keywords Multibody dynamics · Cross-country skiing · Skating technique · Modeling · Experimental verification

✉ John Bruzzo
john.bruzzo@lut.fi

¹ Laboratory of Machine Design, Lappeenranta University of Technology, P.O.Box 20, 53851 Lappeenranta, Finland

² Laboratory of Engineering Mechanics, Faculty of Mechanical Engineering 3mE, Delft University of Technology, Mekelweg 2, 2628CD Delft, The Netherlands

³ Department of Biology of Physical Activity, Neuromuscular Research Center, University of Jyväskylä, Kidekuja 2, 88610 Vuokatti, Sotkamo, Finland

1 Introduction

The importance of skiing in Nordic countries is evident; Lind and Sanders [1] state that this activity has existed as part of daily commuting in that part of the world for more than 6000 years. In modern life, skiing has transformed into a leisure activity and a discipline in major sporting events. Of all the variants and techniques in cross-country skiing, the skating technique can be considered the youngest one, developed roughly 40 years ago, according to Allen [2].

The skating style is the variant of cross-country skiing where the skier's movement resembles that of an ice skater. In skating style, the quality of the technique is of major importance, and poor performance can lead to high physical impact for the practitioner as the way to compensate this lack of flowed movement is by exerting more force during the pushing action.

As the discipline is relatively new, major efforts have been made to understand the technique, but the focus has mainly been on the physiology, medicine and training aspects, as can be seen in the literature review by Bruzzo [3].

In any sport discipline, the participation of experienced coaches is a key factor in enhancing the potential of the athletes. Pensgaard and Roberts [4] agree that it is obvious that the multiple benefits of their toolkit, comprising combined training experience, motivational techniques, and use of advanced measurement devices, can minimize the performance analysis time of different techniques and activities. Nevertheless, the limitations of the current training culture studied by Krosshaug et al. [5] open up an opportunity to incorporate well validated simulation models into this toolkit.

Attempts to develop a simulation model for skiing dynamics have remained a mere description of the

movements performed by the practitioner. In most of the related studies, a great deal is given to the direct measurement of the resultant force exerted by the skier as this has a great influence in the forward speed of the athlete.

In this study, the authors demonstrate the feasibility of mimicking realistic forces and motions in skiing by validating the model with a professional skier. This model will be based on the seminal work in speed skating modeling by Fintelman et al. [6].

Fintelman introduced a speed skater model where the full body of the athlete was represented by three lump masses with their movement contained in two dimensions. Two of these masses represented the skates and the third mass represented the rest of the body concentrated in the center of mass of the skater. The restriction of movement in the skater model is an assumption made because of the natural tendency of the professional athletes to keep the vertical movement of their center of mass within a minimum range. The outcome of this model was the ability to reproduce the trajectories and forces exerted by the speed skater.

In the skier model, the body of the athlete was represented by the leg performing the propulsion and the rest of the body as a lump mass located in the upper end of this leg. The active leg was divided into three parts to simulate as closely as possible the natural joint movements of the skier's leg. Additionally, the movement of the body parts in the skier model are not confined to the plane movement because in skiing, the vertical movement is larger than in the case of the speed skater. Besides all of the above, it could be noticed that the techniques were very close to each other.

From the modeling point of view, the research team was interested in using the positions and velocities of the different points of the skier's lower limb. Then, as no other external forces besides gravity, friction and air drag were applied, the internal forces that the skier exerts while performing the propulsion in one single propulsion phase were calculated. This technique is known as inverse dynamics, where the forces necessary to perform a determined movement are obtained from the experimental kinematic data. This technique is limited because it is customized case by case, that is, for each experimental piece of data used, just one correspondent force output set is obtained.

Additionally, some other limitations are present in this study, such as using estimated values for the friction and air drag coefficient and being constrained to one single propulsion phase.

The novel objective of this paper is to introduce a multibody model that utilizes the kinematic data from a propulsion phase obtained from a motion capture system to calculate the resultant force and thus the propulsion force.

This simulation method avoids the use of force measurement instruments or sensors, enabling the assessment of the athlete's forces outcome with a minimum set of measurement equipment.

To verify the closeness of the results, the resultant force experimentally measured in the same active phase is then used to validate the results produced by the multibody model.

2 Methods

2.1 Approach to the problem

This study focuses on developing a simple mechanical model for simulating and describing the general aspects of the skating technique in cross-country skiing. The use of a simplified model is justified when the output information is obtained within certain broad limits of accuracy, as is shown by Bruzzo et al. [7]. When more accuracy or more detailed information is needed, moving to complex models might seem the path to follow; however, as the model increases its complexity, other complications have to be considered. Among these are the computational burden if the model is used in real-time simulation, precise knowledge of all the needed system parameters and input variables, and the appearance of unknowns which are difficult to estimate correctly and cannot be experimented with (see Liu and Popovi [8]).

The following key aspects were addressed in order to replicate the human movements of the skier:

- the selection of the multibody dynamic theory to develop the equations of motion of the skier model;
- the selection of an adequate representation of the leg of the skier;
- assumptions to simplify the skier's movement;
- the assumption of the skier's resistance forces: friction and air drag;
- the input of the prescribed motion to represent the movement of the lower limb of the skier.

A good reference regarding assumptions and their effect on the modeling of the ski skating technique is Fintelman et al. [6], who modeled speed skating. Although the approach used in this study differs from the one used for the speed skater, the generality of the assumptions may be considered to be of the same type.

2.2 Simulation model

As previously mentioned, some assumptions had to be made in order to achieve a close replica of the human body movements. One of the first assumptions was the selection

of the number of bodies used to represent the leg of the skier. Figure 1 shows the proposed assumptions of the skier's leg. The model has to simulate the natural movement of the leg during the performance of the technique as closely as possible.

The joints between the bodies are modeled as follows. The knee joint is modeled as a revolute or hinge joint. The use of this joint considers only the flexion and extension of the knee during the simulation process. The joint between the lower leg and the ski is modeled as a spherical joint allowing only rotational movements of the ski with respect to the lower leg. Finally, the joint between the ski and the ground will have five restrictions, such that, when on the snow, it is only able to move in the longitudinal or gliding direction of the ski.

As the model will simulate only the phase when one leg is pushing to complete the stride motion towards the gliding leg, just the kinematics of the pushing leg will be considered during the simulation. This transforms the closed loop formed by the ground and the two skier's legs into an open loop formed by the ground and the pushing leg. The effect of the gliding leg is accounted for by including in the model the forces produced by it. This transformation exploits the flexibility of the multibody dynamics formulation and reduces the complexity of the model. Additionally, the relative motions of the upper body with respect to the pushing leg, the arm movement and the orientation of the trunk are also excluded from the simulation model at this stage.

The upper body mass is concentrated at the top of the upper leg. This approach was used previously by Fintelman et al. [6] and Bruzzo et al. [7]. As mentioned by Bruzzo [3], one of the main justifications for this is that the upper body helps to balance the body of the athlete. However, its influence on the kinematic parameters of the movement is not yet clear and for simple models the results fit into the

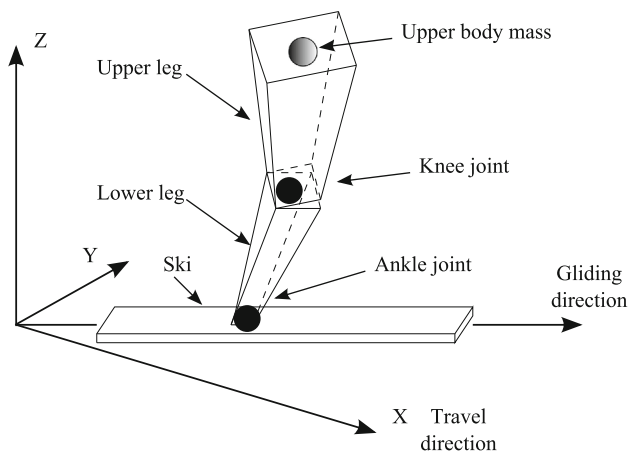


Fig. 1 Simplification of the leg in the skier model

acceptable ranges. The only consideration of the upper body is related to the estimation of the air drag as one of the opposing forces to the movement of the skier. For the present study, it is considered that the ski travels along a straight line and that no skewing or lateral slip in the ski is present.

To illustrate the forces produced during the propulsion phase, Fig. 2 describes the active forces present during this phase.

Rusko [9] proposes that the resultant force exerted by the pushing leg can be divided as the vectorial sum of three main acting forces: the vertical force, the side to side force and the propulsive force. This propulsive force is the component that is actively related to the travel movement of the technique, thus affecting the output speed of the skier. Actions or improvements to increase this force will directly impact the performance of the skier.

Finally, the equations of motion for this model were derived by using the technique of rigid bodies with constraints, and by using a full set of coordinates. Their use and implementation is very straightforward according to Chaudhary and Saha [10]. They are presented as a set of differential algebraic equations that can be integrated using the built-in MATLAB (MATLAB 8.1.0.604, The MathWorks Inc., Natick, MA, 2000) function ODE45 to obtain the velocities and positions of the points on the model that

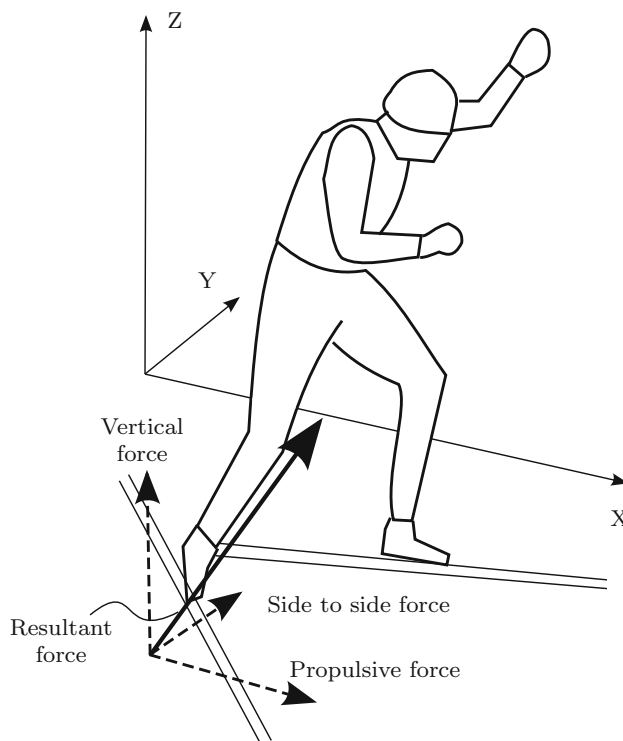


Fig. 2 Forces acting during the propulsion phase. Figure adapted from [9]

researchers are interested in during the simulation. The equations of motion in this form provide information on the type of restrictions imposed by the segment joints and the forces produced to enforce them. These constraint forces are one of the key aspects of this study, as they are the calculated resultant forces exerted by the skier during the propulsion phase. The derivation of the equations of motion and all the detailed components can be found in Appendix 1.

2.3 Skier

A professional skier, a member of the Finnish Olympic team, was the test subject to demonstrate the feasibility and validity of the simple mechanical model. The physiological parameters needed as inputs in the skier model are the mass and height of the skier, and the weight and dimensions of the ski and binding.

The different lengths of the leg segments were taken directly from the distance measurement of the markers positioned on the topological points of the legs (ankle, knee, and head of the femur). However, these data are only used at this stage of development of the model as a validation tool for comparison with simulation outputs. The model itself generates these data based on the physiological studies presented by Yeadon [11]. The purpose of this is to provide the model in the future with some generality to avoid adding more measurement procedures and ease the use of the model as a practical tool by teams with different scopes: high competitions, leisure activities, or beginners.

2.4 Measurement equipment

All of the data were collected in the ski tunnel in the Vuokatti Sports Institute [12]. The length of this indoor ski track is about 1 km with different track steepnesses to perform tests and for skiing in general. The tunnel temperature is normally kept between -5 and -9°C . An update on the conditions of the ski tunnel can be found on the Vuokatti website. All of the snow in the tunnel is maintained mechanically, and also fresh snow can be produced when needed. Due to the restrictions on the measurement length of the motion capture equipment, the test was limited to 16 m. This length allows capturing approximately three complete strokes of the skier.

The equipment can be divided into two important segments: the first is the equipment dedicated to performing the experiment in the tunnel and the second is used to develop the multibody dynamic model and the verification of the results. In the experiments, the Vicon System MX manufactured by Vicon Motion Systems, consisting of 16 cameras, was used to acquire the positions of the 37 markers set on the body. The markers were spheres

attached to the body in the locations shown by Figs. 3 and 4 whose positions were acquired by the motion capture system at a sample rate of 1000 Hz.

To measure the forces exerted by the foot on the ski, an in-house force measurement system was used. The validity of this force system has been reviewed by Ohtonen et al. [13].

This measurement system allows obtaining the full resultant force exerted by the skier. It contains the sum of all the forces produced during the propulsion phase independently of how they are produced. At this stage of development, this feature reduces the need for a detailed analysis of the role of the individual movements and parts of the leg and foot.

The system Protom Light System, Model Con 12 was used as a visual speed indicator for the skier to carry out the test run. It is important to mention that the final velocity used in the model was the real one calculated from the motion capture system data. To collect and transmit the

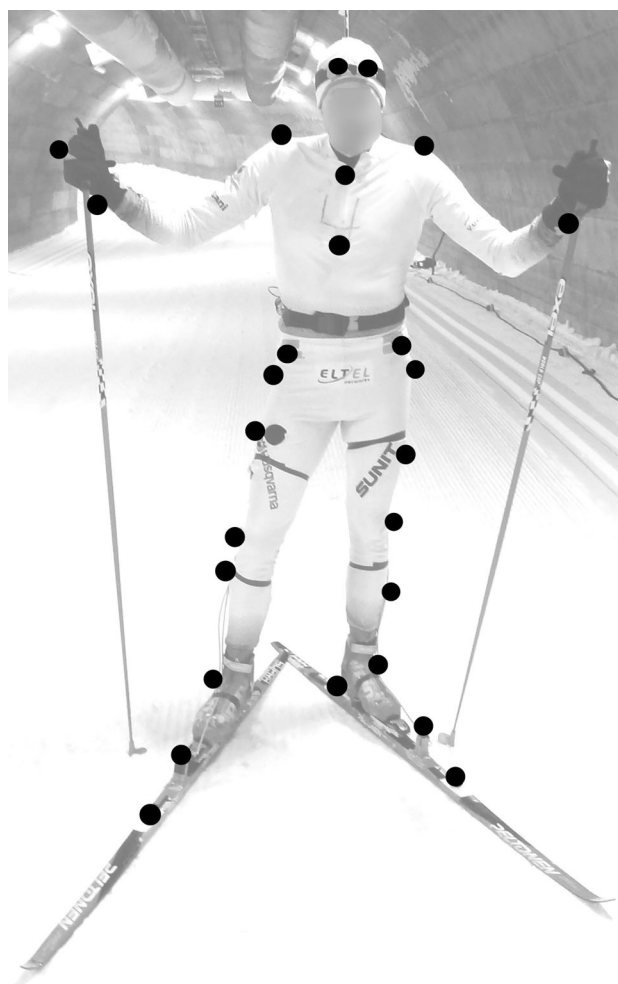


Fig. 3 Markers positioning represented by *black dots*. Frontal view

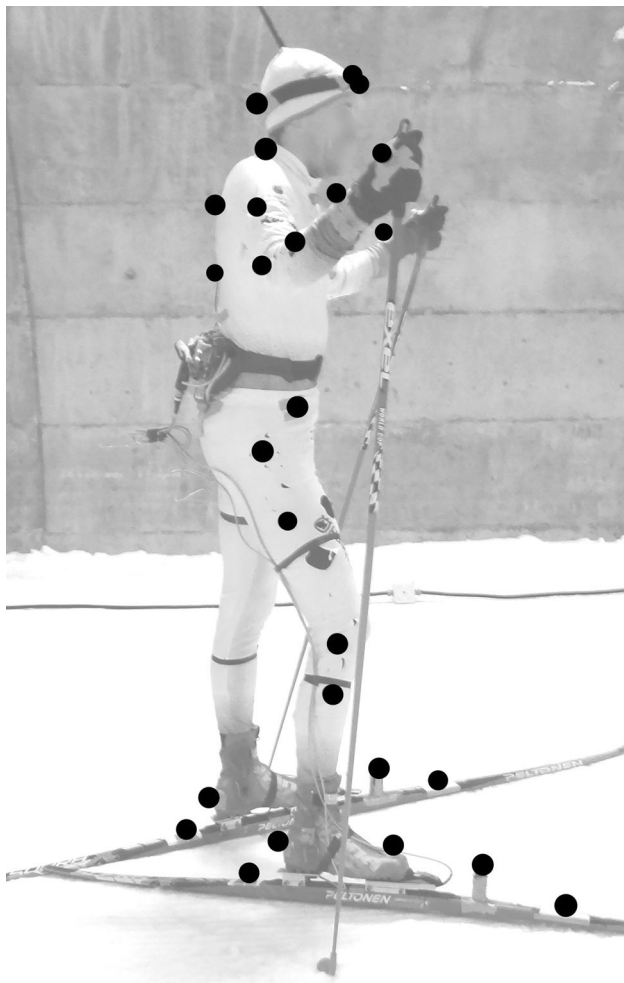


Fig. 4 Markers positioning represented by *black dots*. Lateral view data to the computer used to preprocess the experiment data, the following equipment was used:

- two custom-made small and lightweight (980 g) force plate pairs built by the Neuromuscular Research Center, University of Jyväskylä;
- an eight channel ski force amplifier built by the Neuromuscular Research Center, University of Jyväskylä;
- an A/D converter with a sampling rate of 1 kHz, model NI 9205, National Instruments, Austin, Texas, USA;
- a wireless transmitter WLS-9163, National Instruments, Austin, Texas, USA;
- a PC laptop with a wireless receiver card and data collection software LabVIEW 8.5, National Instruments, Austin, Texas, USA.

The final weight of the measurement and collection system combined with the transmitting system was approximately 2030 g.

To manipulate the motion capture data from the experiments, the MATLAB 2013a software and the Vicon Nexus

software were used, respectively. MS Office was used to preview the result of the measured forces and to apply the necessary calibration offsets and conversion constants.

2.5 Measurement procedure

The measurement system was configured, set and calibrated according to the manufacturer's recommendations, and the force measurement system was calibrated using the internal existent protocol of the Neuromuscular Research Center of the University of Jyväskylä. Further specifications of the measuring system can be found in the work of Ohtonen et al. [13].

The test subject did not perform any structured warm-up prior to performing the tasks; however, the one kilometer skiing run to reach the test zone inside of the tunnel can be considered a warm-up. No other exercises were needed to get used to the equipment, as the same test subject has performed this test many times in the past. Then, a specific skiing speed was set as the only parameter to be followed by the skier (using a set of pacing lights along the track) during the execution of the skating technique without poles. The forward speeds used in the test were 5 and 6 m/s. For each specified speed, three runs were made to ensure the availability of clean raw data.

All of the marker positions and force data were collected and saved in usable formats to be input in the simulation model. The motion capture data were exported in the .c3d format and in the case of the force, the format used was .txt. No synchronization issues between the position capture and force data appeared thanks to the Vicon Nexus software linking these two sets. After selecting the information of the markers to be input into the model, the forces exerted by the foot on the ski were calculated and compared against those measured with the force acquisition system.

The friction and air drag coefficients were taken from the literature (Kiroiwa [14] and Chen and Ki [15]) and not measured from real conditions at this time. It is worth mentioning that, although the friction coefficient is one of the most variable parameters that an athlete can encounter while skiing, this test focused on the movement of the leg more than the conditions of the surrounding environments. The controlled conditions of the ski tunnel in Vuokatti allows concentrating on this. In the next versions of the models, the plan is to increase the complexity of the experiment by measuring and adding the actual values of snow-ski friction.

2.6 Data analysis

The data needed some preprocessing to make it suitable for use in the model. Firstly, the data belonging to the selected

propulsion phase was isolated from the rest of the measurements. This was done by analyzing the marker positions attached to both skis and the positioning of the center of mass of the skier with respect to each ski. Finally, a comparison of the measured force from each binding clarified which leg was pushing and which one was gliding. Only the position and force data of the leg performing the propulsion was taken.

Secondly, as the multibody model needs to use the position of the selected lower limb markers to extract the respective Euler angles of the leg parts, it was important to guarantee that these functions representing the Euler angles were smooth, continuous and differentiable up to the second degree. A Fourier fitting process was then used to convert the discrete data into continuous functions. Finally, to verify that the fitted continuous functions represented the discrete data well, the Pearson correlation coefficient, the analysis of residuals, and the Bland–Altman plots were used to test the goodness of fit.

Figure 5 compares the resultant force raw data and the fitted result. Figure 6 shows the resultant residuals after the fitting process.

It can be seen from Fig. 6 that a large percentage of differences encountered in the fitted function are between -10 and 10 N.

It is also important to show the fitted data used as an input in the model. Figure 7 presents one of the measured Euler angles representing the orientation of the upper leg during the analysis. Next, Fig. 8 presents the residual product of this fitting process. Also the good agreement of the raw versus fitted data can be seen here.

In summary, the simulation process in this paper can be broken down into three main parts as presented in Fig. 9.

In this study, it is not possible to show error bars on the uncertainties of the measurements. The force and position measurements for different test runs cannot be compared because of the high variability of the skier’s movement in the track trial, the lack of a well-established reference point

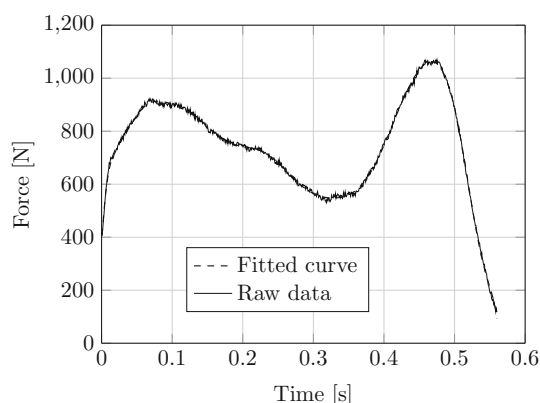


Fig. 5 Comparison of the raw force data and fitting results

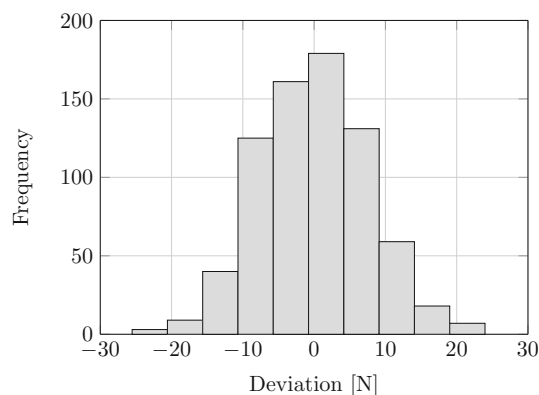


Fig. 6 Histogram of the residuals related to the fitting process of the force

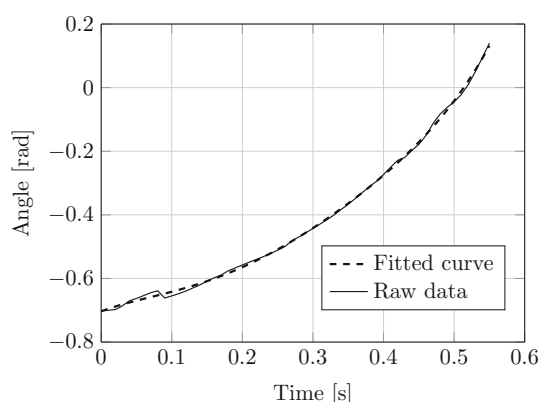


Fig. 7 Comparison of the raw kinematic data and fitting results of one of the Euler angles used to represent the orientation of the upper leg

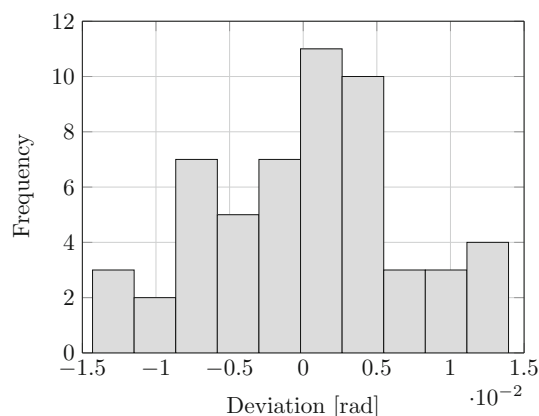


Fig. 8 Histogram of the residuals related to the fitting process of the kinematic data

for comparison and the multiple changes that the skier could introduce with slight changes in technique. Each measurement has to be taken as an individual set of data that could be used in the model. However, the force

measurement system is validated and showed minimal differences to reference systems in various test situations, which can be seen in the work by Ohtonen et al. [13].

3 Results

After inputting the positions measured during the propulsion phase as a reference, the first important simulation output to show is the comparison of the measured and modeled trajectories of three specific topological points on the leg. This comparison validates the response of the model that uses movement simplifications for the leg joints, meaning that it is possible to keep the generality of the leg movements with the assumptions made.

Figure 10 shows the x–y plane projection of the position of these simulated and measured points, and Fig. 11 presents the x–z plane projection.

A simple visual inspection reveals the similarities between the trend of the measured and simulated points on the lower leg. A difference exists also in the trajectory of the points: one reason is that even though the markers of the data acquisition movement are attached to the body, these still have some relative movement that affects the measurement of the position of those points. This was determined when the assumed constant distance between the reference markers was investigated. These marker errors are a common issue to deal with in movement analysis experiments. As presented by Andersen [16], where close accuracy of the measurement is needed, corrective actions have to be enforced.

In Table 1, the Pearson correlation coefficient is used to find out how well the simulated data describes the

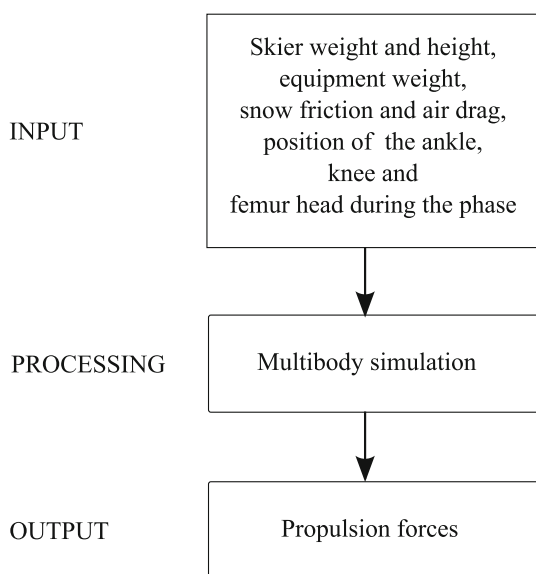


Fig. 9 Simulation process flow chart

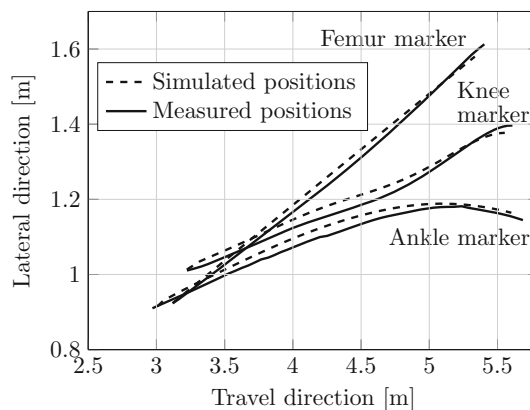


Fig. 10 X–y plane projection of the measured and simulated points for one skiing stroke

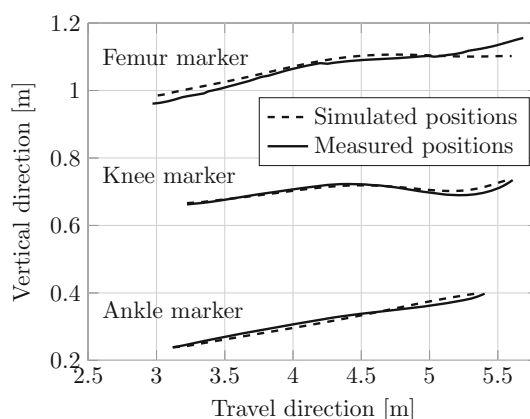


Fig. 11 X–z plane projection of the measured and simulated points for one skiing stroke

Table 1 Pearson correlation coefficient of the position simulated results

	Ankle marker	Knee marker	Femur marker
Plane X–Y	0.9537	0.9927	0.9997
Plane X–Z	0.9724	0.9338	0.9410

experimental data. The closer this value is to one, the better the description of the phenomena is by the simulated data. It can be seen that the values obtained for each case are in good agreement with the expected results.

A comparison between the measured and calculated forces is shown in Fig. 12. Although differences are expected to occur because of the assumptions and simplifications made, the results are still in agreement with the measured data.

In Fig. 12, a simple inspection shows that the simulated force follows a trajectory similar to the measured force. For the present case, the shapes of the curves are very similar with a dwell around $t = 0.35$ s, and a clear push around

$t = 0.47$ s (with an overall Pearson correlation of 0.94). The mean values are approximately the total weight of 785 N of the skier and the maximum difference between the measured and calculated values is about 363 N occurring at around 0.27 s.

As the Pearson correlation coefficient by itself is not enough to assess the agreement between the experimental and simulated set, Fig. 13 introduces the Bland–Altman plot of the comparison of the two time series data representing the resultant force.

From Fig. 13, it can be seen that despite a negative bias, most of the points are within the 95 % confidence interval. This shows that there is a difference between the methods compared; however, the fact that most of the points are scattered inside of the agreement interval can be considered as an acceptable agreement between the simulated results and the measured data.

This level of proximity in the results might be considered as one of the key aspects towards certifying the validity of the proposed model.

Finally, the experimental and simulated resultant forces are projected onto the X, Y, and Z axes to obtain the propulsive, lateral, and vertical force components which are shown in Figs. 14, 15, 16, respectively.

In the case of the propulsion force, Fig. 14, the shape obtained in this figure is close to the one obtained by Fintelman et al. [6] in the speed skater model. Additionally, it can be seen that both, measured and simulated forces, follow a similar path with coincident position of peak values.

A similar case occurs when comparing the lateral forces. In Fig. 15, it can be seen how well the shape of both experimental and simulated curves resemble each other.

While propulsion and lateral forces may have similarities in their shape, the vertical force resembles the shape of the resultant force as it can be noticed in Fig. 16.

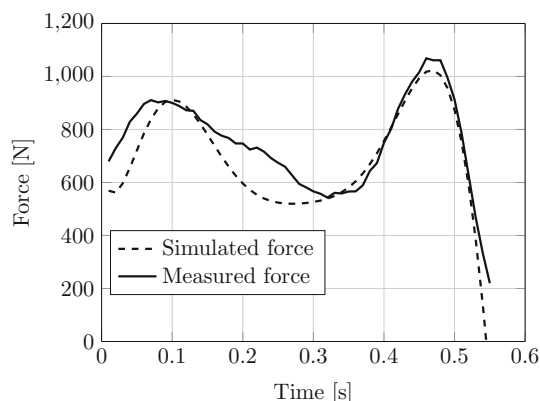


Fig. 12 Comparison of the simulated and measured resultant forces for one skiing stroke.

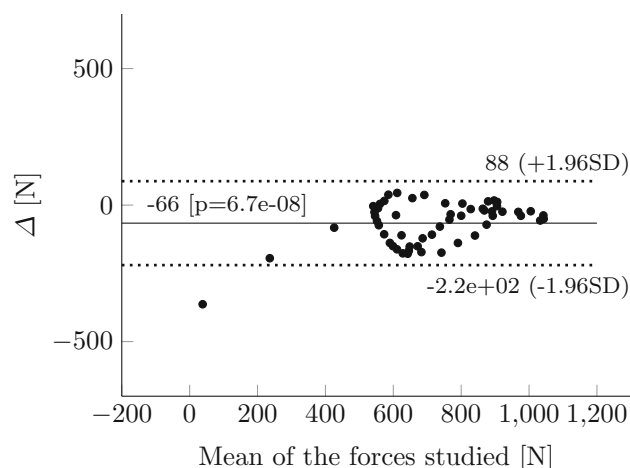


Fig. 13 Bland–Altman plot showing the 95 % limit of agreement between the measured and simulated resultant force

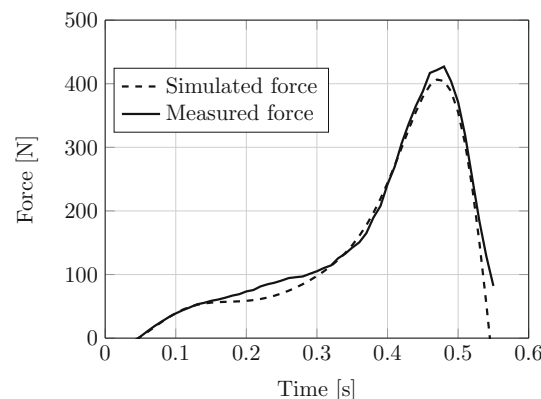


Fig. 14 Simulated and experimental propulsion force for the selected active phase

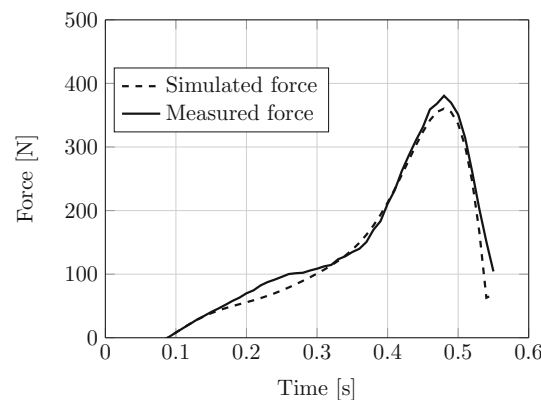


Fig. 15 Simulated and experimental lateral forces for the selected active phase

The information provided by the components of the resultant force is made obvious when looking at their shapes. Propulsion and lateral forces clearly indicate the

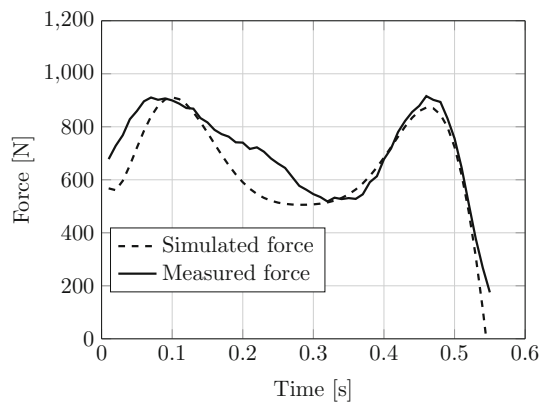


Fig. 16 Simulated and experimental vertical forces for the selected active phase

propulsion moment represented by the peak at the end of the movement. The vertical force contains the information of three important phases during the stroke.

These phases might be defined as follows: the initial touch of the ski represented by the first peak value. The gliding phase denoted by the valley of the curve and finally, the propulsion phase described by the second peak value towards the end of the curve.

4 Discussion

Simulation models can be used in training, technique research, and the development of new equipment. Additionally, the advantages that human models are countless in the investigation of injuries in sports.

This study presented a mechanical model for a skier performing the skating technique in cross-country skiing. The selections of the joints used to model the human movements are, at the same time, simple to implement but also general enough that they cover a wide range of movements included in the natural physiology of the leg. To present an additional advantage of simulation models, Fig. 17 shows a timed visualization of the sequence of leg movements during the propulsion phase.

Visualizations facilitate the analysis process and add relevant information that a mere numeric chart or table cannot present openly to the user. Visualization and movement animation is a well-recognized feature that is used more and more in biomechanics study cases. For example, in the visualization figure, it is simple to observe the bodies forming the leg, the position of the joints and the travel direction of the ski. Also, the flexion and rotation movements can be identified. Another important aspect of this model is the fact that certain parameters that have a high impact on the technique can be changed easily. Track steepness, athlete data, snow friction, and air drag can be

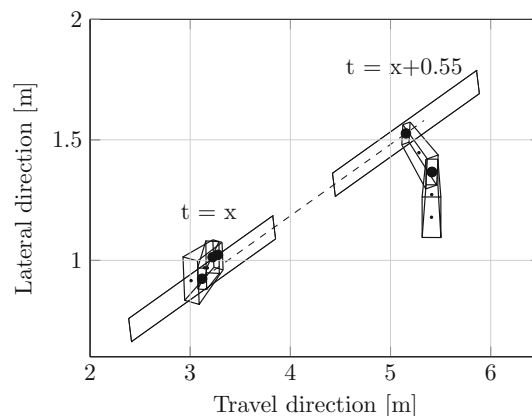


Fig. 17 Leg extension sequence obtained from the multibody skier model. The subsequent time frames are 0.55 s representing the first and last frames

changed very quickly, and a new simulation set is ready to be performed.

The research team considered it convenient to implement the anthropometric data found by Yeadon [11] in the model. The aim behind the use of this type of statistical representation relies on the simplicity that the research team wants to achieve. Counting on a model that minimizes the amount of input data and continues to give close enough results approximates this research to what a simple model should be. Movement and force representation, movement details on the joints of the lower leg during the execution of the phase, and a wide range of visualization speeds guarantee that the customization of the post-processing will fit the requirements of the user.

As the model presented had the objective of resembling the trajectory of certain representative points during a single stride and of determining the forces exerted by the skier on the ski from them, the simplifications and assumptions made were adequate to accomplish the task. The research team proposes that the level of complexity or amount of detail of this model is sufficient to cover the objectives postulated in the introduction section. However, the model may be adjusted and customized for more detailed applications and other areas of study. For example, the only parameter assumptions made in the present case were related to the determination of the snow friction and air drag. These parameters were tuned in an iterative form, but always kept within the limits proposed in the literature.

It is important to mention the limitations of the present model. This study focuses on modeling one skiing stroke without the use of poles. Although this might seem a significant limitation, it is instead the starting point of a more complete modeling system where a complete race could be simulated or reproduced. Advances in wireless technology and miniaturization will, in the near future, enable taking information related to force production, speed or rhythm

automatically from athletes during a competition. This information and the results can be used to enhance the accuracy of the simulation model towards the point where the simulation of a race can become reliable and several scenarios could be analyzed.

Currently, the limited availability of position measuring devices for longer runs with enough accuracy affects the development of other simulation attempts directly. It could be possible to extend the amount of data collected for one short experiment. However, the variability of the skier's movement while performing the technique rapidly prevents the idealization of the model.

It is proposed, as a future step, to work towards the development of this type of reliable equipment, to elaborate more general models, factoring in simulations for the athlete's fatigue, to verify how well this model is able to predict forces and motions of non-professional skiers, and to work on the development of user-friendly interfaces where the coaches, practitioners, and public in general could benefit from these models without the participation of a multibody specialist.

One specific task where this simulation tool can be used is in understanding how the propulsion force is produced taking advantage of the measured kinematic data. In the ski skating style, technique is a key factor to achieve faster and fluid skiing. As it can be seen in the book written by Rusko [9], there exist many elements to be controlled while performing the ski skating style—some of them are done intuitively and others can be learned and reinforced by training.

This tool would allow producing the kind of information to be used in the development stage of athletes. For example, the technique of an inspiring athlete/a young athlete can be compared with that of a top level athlete, enabling the detection of important differences by using a simulation tool. Additionally, a baseline of the practitioner's parameters can be generated to be compared later with the improvement of their practice, and force variations caused by modifications in the leg movement of the athlete can be simulated quickly without the need for field measurements.

5 Conclusion

A simulation tool that could help coaches or researchers in general during the training phase can expedite improvement and serve as a means to evaluate the performance of athletes. This study demonstrated the possibility of using simplified multibody models to simulate the human movement specifically in winter sports such as cross-country skiing.

Even though this is a simple model where the upper mass of the skier's body was positioned in the point

representing the femur, the results obtained on the calculated motion and forces are in good agreement with those measured.

Extending the model with the usage of poles to analyze poled cross-country skiing is a challenging direction for future work.

Appendix 1

Form of the model's equation of motion

In this appendix, the general form of the equation of motion of the skier model is presented and expanded in a detailed manner for terms specific to this case, such as the constraint equations and vector of external forces.

An augmented formulation to account for the knee and ankle joints is employed in this study. The complete development of the augmented formulation can be found in a study by Shabana [17]. Under this formulation, the resultant equation of motion of the dynamic model for one leg on a single propulsion phase can be written as

$$\begin{bmatrix} \mathbf{M} & \mathbf{C}_q^T \\ \mathbf{C}_q & \mathbf{0} \end{bmatrix} \begin{Bmatrix} \ddot{\mathbf{q}} \\ \boldsymbol{\lambda} \end{Bmatrix} = \begin{Bmatrix} \mathbf{Q}_e + \mathbf{Q}_v \\ \mathbf{Q}_d - 2\alpha(\mathbf{C}_q \dot{\mathbf{q}} + \mathbf{C}_t) - (\beta^2)\mathbf{C} \end{Bmatrix} \quad (1)$$

where \mathbf{M} is the mass matrix of the system, \mathbf{C} is the vector of constraints, \mathbf{C}_q is the Jacobian matrix of the constraints, $\ddot{\mathbf{q}}$ is the vector of generalized accelerations, $\boldsymbol{\lambda}$ is the vector of Lagrange multipliers, \mathbf{Q}_e and \mathbf{Q}_v are, respectively, the vector of external forces and the quadratic velocity vector, \mathbf{Q}_d is the vector that arises after taking the second differentiation of the vector of constraints, and finally, α and β are the Baumgarte stabilization parameters used to enforce the imposed constraints. Flores, Pereira, Machado and Seabra [18] propose a method for determining the value of these parameters.

One of the key terms that allows for the determination of the positions and orientations of the different points and segments of interest of the simulated leg is the vector of generalized coordinates, described using

$$\mathbf{q} = \{ \mathbf{q}_1^T \quad \mathbf{q}_2^T \quad \mathbf{q}_3^T \}^T \quad (2)$$

Differentiating this vector twice, the generalized accelerations required in the formulation of the model appear. For the skier model, each term of the vector of generalized coordinates has the form

$$\mathbf{q}_i = \{ R_1^i \quad R_2^i \quad R_3^i \quad \varphi^i \quad \theta^i \quad \psi^i \}^T, \quad i = 1, 2, 3 \quad (3)$$

In Eq. 3, i represents the bodies of the model, $R_{1...3}^i$ are the translational coordinates of the origin of the body reference

system and $\varphi^i, \theta^i, \psi^i$ are the Euler angles used to represent the orientation of the body reference system.

The Euler angle sequence used is $Z_1X_2Y_3$. This specific sequence enables the introduction of the skewing or carving of the ski while the propulsive force is acting in future versions of the model. To facilitate the comprehension of the body reference orientation, Fig. 18 is introduced.

Additionally, Fig. 19 describes of the active propulsion phase that is being simulated. This figure shows the skiing direction, enforced by one system constraint. One of the most important measurable parameters in skiing also appears. This parameter, the angle φ^1 , can also be referred to as the skating angle.

The next term to be fully described is the vector of constraints

$$\mathbf{C} = \{C1 \ C2 \ C3 \ \dots \ C17\}^T \quad (4)$$

which makes possible to enforce the relative movement conditions between the different bodies of the system. Each

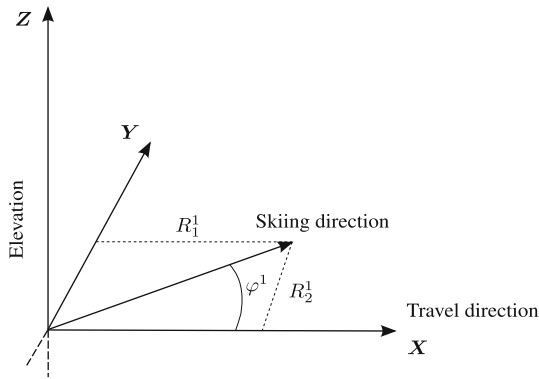


Fig. 19 Description of the active phase basic geometry

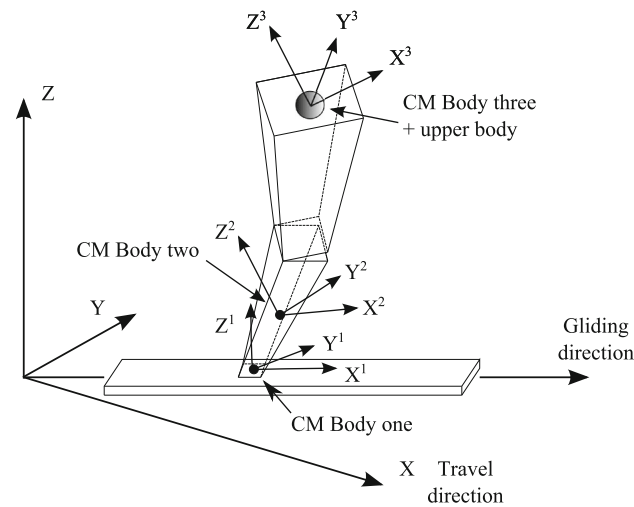


Fig. 18 Body reference system location and orientation

of the member of this vector will be presented sequentially in the following paragraphs.

The first set of five constraints to be defined is the one relative to the ski-ground contact. To specify the steepness of the tracks (leveled, unlevelled with a fixed angle or variable), constraint C1 is written as

$$C1 = R_3^1 - f_3^1(t) = 0 \quad (5)$$

In the constraint equation C1, the term $f_3^1(t)$ is a time function that models the change in elevation of the skiing track. For this specific case, the steepness of the track was put in function of time; however, this constraint could be defined in function of the travel of the skier.

The assumption of the ski traveling in a straight line at an φ^1 angle is enforced by the use of constraint C2. This trigonometric constraint is written as

$$C2 = R_1^1 \sin \varphi^1 - R_2^1 \cos \varphi^1 = 0. \quad (6)$$

The constraint enforcing the constant value of the skating angle is described by

$$C3 = \varphi^1 - c_{\varphi^1} = 0. \quad (7)$$

In this equation, the term c_{φ^1} represents the desired constant value set for the simulation. For the model, the skating angle was taken as the average measured angle from the motion capture system.

To specify the two remaining orientation angles, constraints C4 and C5 are presented next

$$C4 = \theta^1 - c_{\theta^1} = 0 \quad (8)$$

$$C5 = \psi^1 - c_{\psi^1} = 0 \quad (9)$$

In these equations, the constant terms c_{θ^1} and c_{ψ^1} are used to define these constant angle values.

The next constraints C6, C7, and C8, are those related to the union point between the ski and the ankle joint. This joint was considered as a spherical connection, which in a simple form reproduces the allowable movements of the human ankle. This set of three constraints can be written in vector form as

$$\begin{cases} C6 \\ C7 \\ C8 \end{cases} = \mathbf{R}^1 + \mathbf{A}^1 \bar{\mathbf{r}}_p^1 - \mathbf{R}^2 - \mathbf{A}^2 \bar{\mathbf{r}}_p^2 = \mathbf{0}^T \quad (10)$$

In Eq. 10, the terms \mathbf{A}^1 and \mathbf{A}^2 are the rotation matrices that describe, respectively, the orientation of the systems representing the ski and the lower leg with respect to the inertial coordinate system of the system. The vectors $\bar{\mathbf{r}}_p^1$ and $\bar{\mathbf{r}}_p^2$ are, similarly, the position vector of the ankle joint with respect to the origins of the body reference systems described on the body basis.

As the rotational movements of the lower leg with respect to the ski have to be prescribed and have to

reproduce those taken from the motion capture system, constraints C9, C10, and C11 described next are used

$$C9 = \varphi^2 - \varphi_{\text{fitted}}^2(t) = 0 \quad (11)$$

$$C10 = \theta^2 - \theta_{\text{fitted}}^2(t) = 0 \quad (12)$$

$$C11 = \psi^2 - \psi_{\text{fitted}}^2(t) = 0 \quad (13)$$

where $\varphi_{\text{fitted}}^2(t)$, $\theta_{\text{fitted}}^2(t)$, and $\psi_{\text{fitted}}^2(t)$ are the prescribed Euler angles that the body reference system has to follow.

Several approaches exist for modeling the knee joint. In this approach, the joint is described by constraints C12 to C16 as a revolute joint and they are found using

$$\begin{cases} C12 \\ C13 \\ C14 \end{cases} = \mathbf{R}^2 + \mathbf{A}^2 \bar{\mathbf{r}}_o^2 - \mathbf{R}^3 - \mathbf{A}^3 \bar{\mathbf{r}}_o^3 = \mathbf{0}^T \quad (14)$$

$$C15 = \mathbf{r}_1^{2T} \mathbf{r}_2^3 \quad (15)$$

$$C16 = \mathbf{r}_3^{2T} \mathbf{r}_2^3 \quad (16)$$

In Eq. 14, \mathbf{A}^3 is the rotation matrix that describes the orientation of the upper leg with respect to the inertial coordinate system. The vectors $\bar{\mathbf{r}}_o^2$ and $\bar{\mathbf{r}}_o^3$ are, similarly, the position vector of the knee joint with respect to the origins of the body reference systems described on the body basis.

In Eqs. 15 and 16, the terms \mathbf{r}_1^2 , \mathbf{r}_2^3 and \mathbf{r}_3^2 are the unit vectors fixed on the body reference systems that allow imposing the orthogonal conditions of the knee joint.

Finally, constraint C17 describes the imposition of the prescribed knee angle to the model.

$$C17 = \psi^2 - \psi_{\text{fitted}}^2(t) = 0, \quad (17)$$

where $\psi_{\text{fitted}}^2(t)$ is the reference value that the angle ψ^2 has to follow.

After describing the set of 17 constraint equations, it is now possible to show that the resulting number of degrees of freedom of the model is one.

Mass matrix of the system

The construction of the mass matrix of the system will not be fully shown in this report. However, it is important to mention that the inertia components of the different body parts included in the model (lower and upper leg) are taken from previous studies that collected these physiological data. More detailed information can be found in the work of Yeadon [11].

Vector of generalized forces

The vector of generalized forces applied to the skier's model can be interpreted as a combination of three

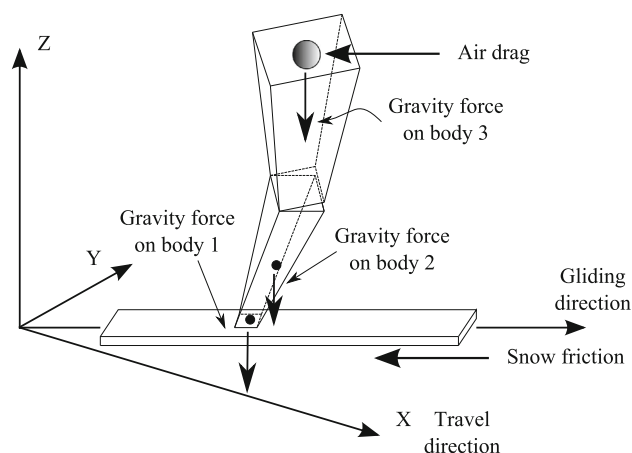


Fig. 20 External forces considered in the skier model

different external forces acting upon the bodies that form the model. Figure 20 presents the external forces on the model and their direction of application.

The first force acting on the three bodies is caused by gravity, the second one is the snow–ski friction that opposes the linear movement of the skis, and the last one is the air drag which is mainly influenced by the frontal area of the skier opposing the direction of movement. These forces have to be converted into generalized forces to be used in the model.

The snow–ski friction transformed into a generalized force can be written as

$$\mathbf{Q}_e^1 = \mathbf{A}^1 \bar{\mathbf{F}}_{\text{friction}}^1 \quad (18)$$

and for the case of the air drag is

$$\mathbf{Q}_e^3 = \mathbf{A}^3 \bar{\mathbf{F}}_{\text{air}}^3, \quad (19)$$

where $\bar{\mathbf{F}}_{\text{friction}}^1$ and $\bar{\mathbf{F}}_{\text{air}}^3$ are the friction force and air drag force, respectively.

The magnitude of the friction force, F_{friction} can be described as

$$F_{\text{friction}} = -\mu F_{\text{normal}}, \quad (20)$$

where μ is the friction coefficient that according to Colbeck [19], can range for snow between 0.05–0.2, and F_{normal} is the normal force that the skier applies against the ground. In this case, the value of the friction coefficient was 0.15.

It is important to mention that this simplified friction model was preferred because of the high complexity of the ski–snow interactions. For this simple model, including the influence of the many variables involved in the formulation of the friction behavior would divert the present study from its main objective. A more complete friction modeling could be included in future versions of the multibody simulation model.

Table 2 Parameters used in the model

Parameter	Value	Units
Mass of the skier	80	kg
Weight of the skis plus force bindings	24	N
Length upper leg	0.4288	m
Length lower leg	0.4489	m
Height of the skier	1.83	m
Coeff. of friction	0.15	
Air drag coeff.	1	
Integration time	0–0.55	s
ρ_{air} @ -5°	1.316	kg m ⁻³
Track vertical change	0.28891	ms ⁻¹
Skating angle φ^1	16.5	o

In the case of the air drag force, F_{air} , the magnitude of this term can be described as follows:

$$F_{\text{air}} = -\frac{1}{2} C_d A_{\text{sk}} \rho v^2, \quad (21)$$

where C_d is the air drag coefficient ranging from 1 to 1.3, A_{sk} is the frontal area of the skier facing the movement, ρ is the air density at the test location temperature, and v is the frontal velocity of the skier. Because of the closed conditions of the ski tunnel where the test was carried out, the lowest value of the air drag coefficient was used, i.e., $C_d = 1$.

The rest of the parameters are developed according to the multibody dynamic theory. For more detailed information on the development of multibody dynamic equations for the skiing technique, please refer to the study presented in the Master's thesis by Bruzzo [3].

Parameters used in the model

Table 2 presents the parameters used to produce the results in this paper in detail.

Appendix 2

Fourier fitting process

In order to obtain smooth continuous functions from the discrete data, which will be used as prescribed inputs in the model, a Fourier fitting process is applied. The basic Fourier relationship to perform this task was found using

$$y(i) = a_0 + \sum_{k=1}^m (a_k \sin(k t w) + b_k \cos(k t w)) \quad (22)$$

where y represents the new set of fitted data or expected value of the unknown, m is the total number of Fourier coefficients performing the fitting, w , a_0 , a_k , and b_k are the Fourier series coefficients, and t is the time step size of the

Table 3 Fitting coefficients of the measured orientation of body 2 represented by its Euler angles

Coeff./angle	φ^2	θ^2	ψ^2
w	5.712	4.423	-0.61263
a_0	-0.07918	0.8879	89,211.1
a_1	0.08884	-1.102	-131,886.4
b_1	0.05972	-0.8758	26,156
a_2	0.01979	-0.1409	50,439.6
b_2	-0.016	0.6811	-20,780
a_3	-0.005422	0.1544	-7764.1
b_3	-0.006807	-0.08529	5134

Table 4 Fitting coefficients of the measured orientation of body 3 represented by its Euler angles

Coeff./angle	φ^3	θ^3	ψ^3
w	2.382	4.423	-0.2854
a_0	1.199	0.06342	266,312
a_1	0.2573	0.165	-408,046
b_1	-3.685	0.347	-102,584
a_2	-2.117	0.1369	173,487
b_2	1.835	-0.354	81,323
a_3	0.7546	-0.1133	-31,755
b_3	-0.05677	0.07081	-20,021

capture process. Tables 3 and 4 show the Fourier fitting coefficients used to smooth the orientation of the bodies representing the lower and upper leg, respectively.

To obtain an idea of how good the fitted function is, the Pearson correlation coefficient r_{xy} is calculated in the way specified next

$$r_{xy} = \frac{n \sum x_i y_i - \sum x_i \sum y_i}{\sqrt{n \sum x_i^2 - (\sum x_i)^2} \sqrt{n \sum y_i^2 - (\sum y_i)^2}} \quad (23)$$

In the equation of the correlation coefficient, the terms x_i and y_i are the sets of data to be compared, and n is the number of collected or calculated data.

References

- Lind D, Sanders SP (2004) The physics of skiing: skiing at the triple point. In: David L, Scott PS (eds) vol 42, 2nd edn, New York, ISBN 9781441918345
- Allen JB (2007) The culture and sport of skiing: from antiquity to World War II. Univ of Massachusetts Press, ISBN 9781558496002
- Bruzzo J (2012) A multibody dynamics model of the cross - country ski-skating technique. Master thesis, Lappeenranta University of Technology

4. Pensgaard AM, Roberts GC (2002) Elite athletes' experiences of the motivational climate: the coach matters. *Scand J Med Sci Sport* 12(1):54–59
5. Krosshaug T, Andersen TE, Olsen OEO, Myklebust G, Bahr R (2005) Research approaches to describe the mechanisms of injuries in sport: limitations and possibilities. *Br J Sports Med* 39(6):330–339
6. Fintelman DM, den Braver O, Schwab AL (2011) A simple 2-dimensional model of speed skating which mimics observed forces and motions. In: *Multibody dynamics, ECCOMAS Thematic Conference*, Brugge, Belgium
7. Bruzzo J, Schwab AL, Mikkola A, Ohtonen O, Linnamo V (2013) A simple multibody dynamic model of cross-country ski-skating. In: *9th International conference on multibody systems, nonlinear dynamics, and control*, ASME, Vol 7A, Portland, Oregon
8. Liu CK, Popović Z (2002) Synthesis of complex dynamic character motion from simple animations. *ACM Trans Graph* 21(3):408–416
9. Rusko H (2003) *Cross country skiing*. Blackwell Science, Malden, Mass, ISBN 9780632055715
10. Chaudhary H, Saha SK (2008) Dynamics and balancing of multibody systems. In: *Lecture notes in applied and computational mechanics*, Springer, Berlin Heidelberg. ISBN 9783540781790
11. Yeadon MR (1990) The simulation of aerial movement-II. A mathematical inertia model of the human body. *J Biomech* 23(1):67–74
12. Vuokatti (2013) Vuokatti city Website. <http://www.vuokatti.fi>. Accessed 13 Jan 2013
13. Ohtonen O, Lindinger S, Lemmettylä T, Seppälä S, Linnamo V (2013) Validation of portable 2D force binding systems for cross-country skiing. *Sports Eng* 16(4):281–296
14. Kiroiwa D (1977) The kinetic friction of snow and ice. *J Glaciol* 19(8):141–152
15. Chen L, Qi ZH (2009) A 2-dimensional multi rigid bodies skiing model. *Multibody Syst Dyn* 21(1):91–98
16. Andersen CR (2009) Determination of rigid body registration marker error from edge error. *J Biomech* 42(7):949–951
17. Shabana AA (1998) *Dynamics of multibody systems*. Cambridge University Press, 2nd edn, ISBN 0521594464
18. Flores P, Pereira R, Machado M, Seabra E (2009) Investigation on the baumgarte stabilization method for dynamic analysis of constrained multibody systems. In: *Proceedings of Eucomes 08, the 2nd European conference on mechanism science*
19. Colbeck S (1992) The friction of snow skis. In: *Proceedings of the 1992 international snow science workshop*, Breckenridge, Colorado